

UC Berkeley

UC Berkeley Previously Published Works

Title

Membrane-Assisted Electrochlorination for Zero-Chemical-Input Point-of-Use Drinking Water Disinfection

Permalink

<https://escholarship.org/uc/item/3q062543>

Journal

ACS ES&T Engineering, 2(10)

ISSN

2690-0645

Authors

Ocasio, Daniel
Sedlak, David L

Publication Date

2022-10-14

DOI

10.1021/acsestengg.2c00116

Peer reviewed



HHS Public Access

Author manuscript

ACS ES T Eng. Author manuscript; available in PMC 2023 April 14.

Published in final edited form as:

ACS ES T Eng. 2022 October 14; 2(10): 1933–1941. doi:10.1021/acsestengg.2c00116.

Membrane-Assisted Electrochlorination for Zero-Chemical-Input Point-of-Use Drinking Water Disinfection

Daniel Ocasio,

David L. Sedlak*

Department of Civil & Environmental Engineering, University of California, Berkeley, Berkeley, CA 94720, USA

Abstract

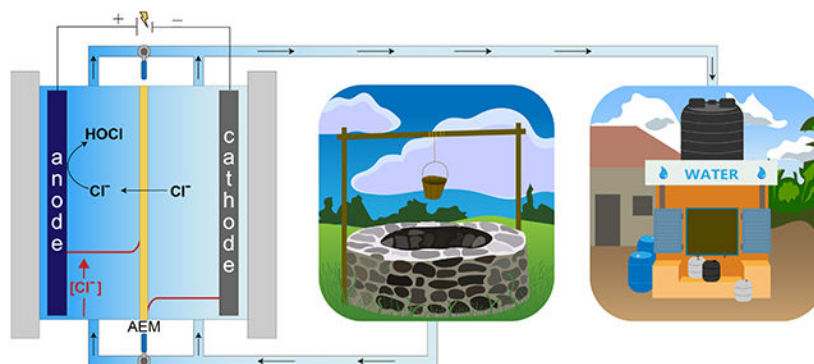
Due to the challenges of providing centralized drinking water infrastructure in low-income and rural settings, point-of-use (POU) disinfection systems are an attractive option for enhancing access to safe drinking water. Electrochlorinators offer an easily scalable and adaptable alternative to POU disinfection systems that require frequent replenishment and accurate dosing of chlorine, but they also require addition of salts on a regular basis. To address this need, we developed an electrochemical disinfection system that efficiently produces chlorine without any chemical inputs. To convert the low concentration of chloride in source waters (i.e., 10–200 mg L⁻¹) to free chlorine (i.e., HOCl/OCl⁻), an anion exchange membrane was positioned between two electrodes, creating two separate chambers. By providing continuous water flow through the catholyte while operating the anolyte in the batch mode, chloride was concentrated into the anolyte, where it was more efficiently converted into chlorine. This approach allowed us to produce chlorine at rates that were about 50% faster than that of an undivided cell operating under similar conditions. Chlorate production was approximately 20% slower in the separated cell compared to an undivided cell; concentrations in finished water never exceeded the World Health Organization's provisional guideline value of 0.7 mg L⁻¹. The performance of the system was further improved by retaining some of the anolyte between operating cycles. This helped avoid periods of high cell potential before salts were concentrated in the anolyte chamber. Use of an anion exchange membrane and a recycled anolyte mode of operation reduced energy consumption by 30%–70% relative to an undivided cell. The energy required to disinfect water ranged from approximately 0.05 to 1 kWh m⁻³, depending on the chloride content and conductivity of the source water.

Graphical Abstract

*Corresponding Author sedlak@berkeley.edu.

Supporting Information

Supporting information is available free of charge at <http://pubs.acs.org>. This information includes a summary of the composition of the studied groundwater and surface water samples; schematics and design information related to the electrochemical cell; data on the formation of chlorine and chlorate production as well as pH changes under different experimental conditions; energy consumption and cell potentials under different operating conditions; information supporting simplified cost estimates; calculations related to the migration and diffusion of chloride in the cells; coulombic efficiencies at different chloride concentrations.



Keywords

Electrochemical chlorine generation; Point-of-use disinfection; Distributed water; Decentralized treatment

1. Introduction

Access to safely managed drinking water supplies expanded from approximately 60% to over 70% of the world's population between 2000 and 2017.¹ However, nearly 2.2 billion people still lack access to safely managed water services.² Nearly half of those lacking basic water services live in low income countries, with 80% located in rural areas where centralized drinking water treatment is difficult to implement.¹ Many others have access to piped water from centralized systems that operate intermittently, necessitating supplemental disinfection or reliance on bottled water. The potential adverse public health outcomes of inadequate water supply systems has led to a growing interest in the development of low-cost decentralized and point-of-use (POU) water treatment systems.³

Although numerous POU and small-scale treatment technologies, including coagulation, media filtration, membrane filtration, and solar disinfection, have achieved adequate disinfection in field trials, there is a need for additional approaches.⁴ Furthermore, in addition to challenges associated with costs and willingness of users to maintain systems, the absence of residual disinfectant in distributed water often leads to post-treatment pathogen contamination during handling and storage.⁵⁻⁷ In many cases, such as with filtration, frequent monitoring and maintenance is required to maintain performance, posing challenges to technology implementation.⁸

In contrast to some of the more complicated approaches, chlorine-based disinfectants provide residual disinfection while offering relative ease-of-use, low cost, and rapid treatment. Most POU chlorinators currently on the market require users to regularly replenish chemical reservoirs either with solid salt tablets (e.g., $\text{Ca}(\text{OCl})_2$) or liquid solutions (NaOCl). Due to the logistical challenge and expense of obtaining solid and liquid forms of chlorine, many users in rural and low-income settings abandon the devices within a few months of receipt.⁹⁻¹¹ For example, rural users exhibited a preference for filtration-based POU devices over consumable chlorine-disinfectants because they believed that the filter

would last, whereas they indicated that they would not need to seek out additional chemicals after their allotted doses of chlorine were depleted.¹²

Electrochemical chlorination technology is a promising alternative POU technology that allows users to generate chlorine from the oxidation of chloride (reactions 1-3).¹³ Results from field studies and life cycle analyses suggest that POU electrochlorinators employed in rural and low-income communities offer operational and economic advantages over direct addition of the disinfectant because NaCl is inexpensive and readily available.^{14,15}



Despite the advantages of electrochemical chlorine generators, the need for users to replenish NaCl may pose similar barriers to adoption and long-term use due to the need for consumable chemicals. NaCl is added to commercially available electrochlorination systems, despite the ubiquitous presence of chloride in water sources, because the efficiency of reaction 1 decreases at low chloride concentrations and low ionic strengths, leading to greater energy consumption and higher operating potentials. To overcome this limitation, we developed an electrochlorination technology that combines approaches from electro dialysis and electrochemical oxidation, whereby chloride present in source waters is converted to free chlorine species without the addition of NaCl by placing an anion exchange membrane (AEM) between two electrodes to create separate anolyte and catholyte chambers. System performance was enhanced by allowing water to continuously flow through the catholyte, while operating the anolyte in the batch mode. To identify the most effective design, two cell configurations were tested under a range of conditions similar to those encountered during POU disinfection. The effect of water composition on chlorine production, energy consumption, and the formation of chlorate also was evaluated.

2. Materials and Methods

2.1 Solutions and water samples

Test solutions (Table 1) were comprised of reagent grade NaCl, Na₂SO₄, and NaHCO₃ (Fisher Scientific, Hampton, NH), with compositions chosen to represent typical Cl⁻, alkalinity, and ionic strength values of groundwater.¹⁶ Variable chloride concentrations were tested to provide insight into system performance under different operating conditions. Surface water samples were collected from San Pablo Reservoir (El Sobrante, CA; 37.916589° N, -122.23279° W) courtesy of East Bay Municipal Utility District Watershed and Recreation. Groundwater samples were taken from a depth of approximately 40 meters from a private well (San Jose, CA; 37.33560° N, -121.73330° W). The composition of the natural water samples is summarized in Table S1.

2.2 Electrochemical cell configurations

A Ti–IrO₂ mixed-metal oxide mesh plate anode (apparent geometric surface area: 8 × 8 cm²; Magneto Special Anodes, Netherlands) was used as the working electrode, accompanied by a stainless-steel mesh cathode (apparent geometric surface area: 8 × 8 cm²; McMaster-Carr, Santa Fe Springs, CA). A square stainless-steel current collector covering the perimeter of the cathode evenly distributed the current. Each electrochemical cell consisted of two square acrylic frames (internal dimensions: 8 × 8 × 0.65 cm³) separated by neoprene rubber gaskets (internal dimensions: 8 × 8 × 0.32 cm³) bolted together between two acrylic side plates (all from McMaster-Carr, Santa Fe Springs, CA). A peristaltic pump (Cole-Parmer, Chicago, IL) coupled with Norprene Tygon A-60-G tubing (Masterflex, Vernon Hills, IL) was used to circulate solution through the system. An anion exchange membrane (AEM) (dimensions: 8 × 8 cm²; Fumasep FAS-PET 130, Fumatech, Bietigheim-Bissingen, Germany) was used in the separated cell configuration (described below) to create distinct anolyte and catholyte chambers of equal dimensions (8 × 8 × 1.3 cm³) (Fig. S1).

The separated cell (Figure 1a) was compared to an undivided cell configuration (Figure 1b). The separated cell incorporated an AEM between the electrodes to create distinct anolyte and catholyte chambers. This allowed for production of a concentrated solution of free chlorine in the anolyte that could be added to the larger volume of water that passed through the catholyte chamber. In the separated cell configuration, water continuously flowed through the catholyte chamber at a rate of 1 mL sec⁻¹ (hydraulic retention time of ~1.4 minutes), while 250 mL of anolyte was recirculated between the chamber and a flask at the same flow rate. The undivided cell had a continuous flow rate of 1 mL sec⁻¹ (hydraulic retention time of ~2.8 minutes) through a single cell compartment in which no membrane was used to separate the electrodes. The interelectrode distance of both cells was 2.1 cm.

2.3 Experimental approach

All electrolysis experiments were performed at room temperature (23 ± 2 °C) in galvanostatic mode, controlled by either a multichannel potentiostat (Gamry Instruments Inc., Warminster, PA) or a power supply (BK Precision, Yorba Linda, CA) when the expected cell potential exceeded the limit of the potentiostat (i.e., 30 V). At least three replicates of each experiment were performed, and error bars represent the standard error on the mean of the replicate experimental data. Initially, the anolyte and catholyte had the same ionic composition. Where appropriate, results were expressed as a function of the applied charge density, ρ_q (C L⁻¹):

$$\rho_q = \int \frac{I(t) \times A}{V} dt = \frac{IA t}{V} \quad (4)$$

where I is current density (A cm⁻²), A is the working electrode surface area (cm²), t is the hydraulic residence time of the anolyte (s), and V is the anolyte chamber reactor volume (L).

Prior to beginning an experiment, the system was flushed with at least 2 L of Milli-Q water and then washed with at least 1 L of test solution. Samples were collected from the anolyte

and the catholyte effluent stream or from the collected effluent basin periodically throughout the experiment. All samples were analyzed for ionic composition and pH. Chlorine measurements were made immediately after diluting samples 5-60 times, depending on the expected chlorine concentration.

Recycled anolyte tests were performed in the separated cell by retaining a portion of the anolyte in the chamber to increase the total cell conductivity with each subsequent cell operation. During these experiments, half of the anolyte volume (125 mL) was replaced with the same volume of feed solution at the beginning of each run. This was repeated until a steady-state condition was achieved (typically within 5 cycles).

The effects of current density on chlorine production were assessed in the separated cell by varying the applied current between 50 mA and 900 mA. The electrolysis period was adjusted to correspond to a final charge density of 2160 C L^{-1} (e.g., 180 min for 50 mA, 10 min for 900 mA). In separate tests, a Ag/AgCl reference electrode was used to measure the anodic interface potential, and values were then adjusted versus SHE. These measurements were taken in an electrolyte of 1.41 mM NaCl, 1.5 mM NaHCO_3 , and 1 M Na_2SO_4 as a background electrolyte to minimize the potential drop in the solution between the reference electrode and the anode.

The effects of variable chloride concentrations (Table 1) and natural waters (Table S1) were investigated in the separated cell at an applied current of 300 mA and 150 mA, respectively. Neither surface water or groundwater feeds were filtered or treated in any manner prior to electrolysis.

2.4 Analytical methods

Free chlorine was measured with a UV spectrophotometer (Vernier, Beaverton, OR) by the *N,N*-diethyl-*p*-phenylenediamine (DPD) (Sigma Aldrich, St. Louis, MO) method.¹⁸ The NaOCl stock solution (Sigma Aldrich, St. Louis, MO) used for the calibration curve was standardized prior to use by $\text{Na}_2\text{S}_2\text{O}_3$ titration. The $\text{Na}_2\text{S}_2\text{O}_3$ solution used for standardization was first standardized by KIO_3 titration. The concentration of the standardized NaOCl stock solution was periodically verified by UV absorbance measurements. Cl^- , ClO_3^- , and SO_4^{2-} were determined using a Dionex DX-120 ion chromatograph with an AS23 column. Na^+ , Ca^{2+} , and Mg^{2+} were analyzed using a Dionex ICS2000 ion chromatograph with a CS12A column (Thermo-Fisher Scientific, Waltham, MA). Dissolved organic carbon (DOC) and total carbon (TC) measurements were taken using a Shimadzu TOC-V analyzer. Statistical significance was determined using ANOVA tests, where the significance threshold was set to $P = 0.05$.

2.5 Energy consumption calculations

The cell potential between the working and counter electrodes was measured in a two-electrode configuration. These measurements were used along with periodic free chlorine measurements to determine the energy consumption E (kWh m^{-3}) of the system:

$$E = \frac{\int I \times V(t) dt}{m_{HOCl}(t)} \times C_{dose} \times 1 \frac{kWh \times L}{Wh \times m^3} \quad (5)$$

where I is the galvanostatic operating current (A), V is the cell potential (V) at time t (hr), m_{HOCl} is the mass of free chlorine (mg) produced at time t , and C_{dose} is the theoretical desired free chlorine dosage (mg L^{-1}). A value of 2 mg L^{-1} free chlorine was selected for C_{dose} based on the World Health Organization's recommendation for household treatment of clear water ($< 10 \text{ NTU}$).¹⁹ A numerical method was used to approximate the integral in equation 5.

3. Results and discussion

3.1 Cell configuration comparison

Two different cell designs were evaluated to assess their effectiveness of chlorine production. The separated cell (Fig. 1a) used an AEM for multiple purposes. First, it inhibited reduction of free chlorine at the cathode by restricting its migration out of the anode chamber. Second, it increased chlorine production rates by concentrating chloride from the catholyte stream into the anolyte. Lastly, it reduced energy consumption by increasing the conductivity of the anolyte. The undivided cell (Fig. 1b) can be considered as a control to benchmark the system to in-line POU electrochlorinators that generate chlorine without the addition of salts.²⁰⁻²³ A third configuration, the “sandwich cell” (Figure S2), was also tested to assess the possibility of achieving the advantages of the separated cell while also eliminating ohmic losses through solution by using the AEM as a solid electrolyte. However, this design did not perform as well as the separated cell. Data for the sandwich cell are included in the Supporting Information (Text S1 and Figures S2-S3).

The addition of an anion exchange membrane in the separated cell significantly increased the rate of free chlorine production compared to the undivided cell ($P = 0.001$) (Fig. 2a), with rates of free chlorine production increasing by approximately 50%. The coulombic efficiency of chlorine evolution of each cell was relatively low due to low initial chloride concentration (i.e., 50 mg L^{-1}). Efficiencies of $10.8 \pm 0.4 \%$ and $7.00 \pm 0.12 \%$ were measured for the separated and undivided cells, respectively. Additionally, the chlorate production rate in the separated cell ($7.34 \pm 1.04 \mu\text{g min}^{-1}$) was 22% lower than in the undivided cell ($P = 0.04$, $9.42 \pm 0.24 \mu\text{g min}^{-1}$) (Fig. S4), despite its higher chloride concentration and free chlorine production rate. Lower chlorate production rates in the separated cell anolyte were likely due to more acidic pH conditions in the anolyte relative to conditions in the undivided cell (a discussion of chlorate formation is presented in section 3.3.1).

The higher free chlorine production rate and coulombic efficiency of the separated cell compared to the undivided cell was due to the higher concentration of chloride in the anolyte chamber (Fig. 2b). The concentration of chloride in the undivided cell did not significantly change throughout the electrolysis period (i.e., it was equal to that of the water undergoing treatment), whereas the concentration of chloride in the separated cell anolyte

nearly doubled. In this manner, the AEM employed electro dialysis to concentrate chloride and other anions in the separated cell's anolyte chamber.

The energy consumption necessary to achieve a disinfectant concentration of $2 \text{ mg Cl}_2 \text{ L}^{-1}$ in the treated water was $0.135 \pm 0.017 \text{ kWh m}^{-3}$ and $0.197 \pm 0.013 \text{ kWh m}^{-3}$ for the separated and undivided cells, respectively. The undivided cell operated at a total cell potential of $9.53 \pm 0.03 \text{ V}$ due to overpotential and ohmic losses in the low conductivity solution (Fig. S5). The separated cell, however, experienced a steady decrease in total cell potential over the course of the experiment, decreasing from $11.64 \pm 0.88 \text{ V}$ to $7.61 \pm 0.56 \text{ V}$ as conductivity in the anolyte chamber increased. The potential was initially higher than that of the undivided cell due to the added resistance of the AEM.

Although the undivided cell design offers simplicity, it was inferior to the separated cell in terms of chlorine production, energy consumption, and chlorate formation in an electrolyte representative of naturally occurring chloride levels and conductivity. It also produced a more dilute free chlorine solution. In addition to higher production rates and lower energy consumption, the separated cell allows the user to produce a concentrated solution of free chlorine that may be added to water according to their needs or may also be used separately as a multi-purpose surface disinfectant.

3.2 Recycled anolyte operation of separated cell

During the initial period of operation, the efficiency of the separated cell was not much higher than that of the undivided cell because chloride concentrations in the anolyte chamber were only slightly higher than those in the source water. A start-up period was required to concentrate chloride in the anolyte and increase the conductivity sufficiently to take advantage of the separated cell's intended design. To minimize this phenomenon, a portion (125 mL) of the relatively high ionic strength anolyte was retained from the previous cycle to increase the initial conductivity during the next cycle of chlorine generation. Under this operating scheme, the initial conductivity of the separated cell's anolyte was about two to three times higher than that of the source water (Fig. S6). By the third cycle, the initial conductivity of the electrolyte was sufficiently high to drive the initial cell potential of the separated cell below the potential of the undivided cell (Fig. 3a). As the initial chloride concentration in the anolyte increased (Fig. 3b), higher free chlorine concentrations were produced (Fig. 3c). The lower potential and higher chloride concentrations resulted less energy consumption in the separated cell after the initial start-up period. For example, by the fourth cycle, the energy consumption was about 45% lower than that of the undivided cell when half of the anolyte was used (i.e., the energy use was 0.11 kWh m^{-3}), and about 72% lower when the entire anolyte volume was added to the water (i.e., 0.054 kWh m^{-3}). The increased chlorine production due to anolyte retention allowed the device to treat 58% more water by the fourth cycle assuming a target chlorine concentration of $2 \text{ mg Cl}_2 \text{ L}^{-1}$.

3.3 Effects of current on chlorine production and energy use

In practice, the rate of chlorine production can be increased by increasing the applied current, but this is likely to lead to an increase in energy consumption. We tested currents ranging from 50 to 900 mA (i.e., current densities ranging from 7.8 to 140 A m^{-2})

(electrolyte conditions listed in Table 1) over electrolysis periods corresponding to a final applied charge density of 2160 C L⁻¹ (i.e., 180 minutes for 50 mA, 10 minutes for 900 mA) in the separated cell (Fig. S7). The difference between the charge-based chlorine production rates (i.e., mg Cl₂ C⁻¹) was not significant among the seven applied currents tested ($P > 0.52$). The average charge-based chlorine production rate for the experimental conditions (i.e., 1.41 mM Cl⁻, 7 mM ionic strength) was 0.034 ± 0.005 mg Cl₂ eq C⁻¹. From this information, the free chlorine production rate can be expressed as a function of applied current:

$$\frac{dm_{Cl_2}}{dt} \approx (2.02 \text{ mg min}^{-1} \text{ A}^{-1}) I \quad (0.05 < I < 0.90 \text{ A}) \quad (6)$$

where $\frac{dm_{Cl_2}}{dt}$ is the rate of free chlorine production (mg Cl₂ min⁻¹) and I is the applied current (A).

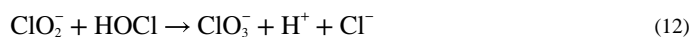
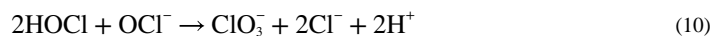
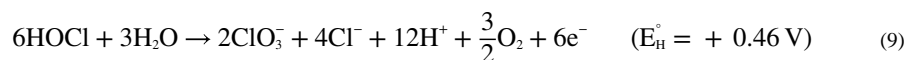
The energy required to achieve an initial concentration of 2 mg Cl₂ L⁻¹ in the storage reservoir that received that disinfectant solution ranged from 0.089 ± 0.013 kWh m⁻³ when 50 mA was applied to 0.60 ± 0.02 kWh m⁻³ when 900 mA was applied (Fig. S8). These large differences can be explained by the wide variation in total cell potential resulting from the different currents (Fig. S9). For example, the cell potential at 50 mA ranged from 6.00 ± 0.33 V initially to 4.14 ± 0.10 V at the end of the electrolysis period, while the observed potential when 900 mA was applied ranged from 44.6 ± 0.8 V to 28.6 ± 0.4 V. From these data we can predict the energy consumption under the same test conditions as a function of applied current:

$$E = (6.13 \times 10^{-4} \text{ kWh m}^{-3}) \times I + (6.51 \times 10^{-2} \text{ kWh m}^{-3}) \quad (50 < I < 900 \text{ mA}) \quad (7)$$

where E is the energy consumption (kWh m⁻³) of the electrochemical cell necessary to chlorinate at a concentration of 2 mg Cl₂ L⁻¹ and I is the applied current (mA). Results from studies on electrochlorination indicate energy values ranging from about 0.01 to 100 kWh m⁻³ for similar chlorine doses.²⁴ The high end of these energy values may be prohibitive for large-scale treatment options in which millions of gallons of water are treated daily, but they may be suitable for small-scale operations that produce only a few liters per day. An economic analysis of small-scale electrochlorination systems at three different rural sites indicated that energy costs were insignificant relative to the initial capital investment and other operation and maintenance costs.¹⁴ One factor that contributed to these findings was that water usage was far less than the design capacity, likely due to users drawing disinfected water mainly for drinking and cooking. A simplified economic analysis of this electrochlorination system in comparison to systems that dose liquid bleach or chlorine from solid tablets yield similar outcomes (Text S2). Over a 10-year lifetime for a system that treats 200 L day⁻¹, the cost due to electrical energy consumption for the electrochlorinator was a less than 5% of the cost of consumable chemicals associated with chemical dosing systems. These findings suggest that the energy requirements of this system will not be prohibitive for small-scale applications.

3.3.1 Effects of current on chlorate formation—Unlike the trends observed for chlorine production, chlorate formation varied with applied current, with production rates increasing from 50 mA to 600 mA, whereafter production plateaued (Fig. 4). The relationship between chlorate production rate and charge density was related to conditions in the anolyte chamber. The stabilization of chlorate production rates at the highest applied current was related to the formation of protons at the anode surface (reaction 8) and from the formation of free chlorine (reactions 1-3). The average pH for each current tested rapidly dropped from 7.75 ± 0.27 to below 5 by the first sampling point, then gradually decreased to 2.6 ± 0.55 over the course of electrolysis, whereas the pH of the catholyte only moderately increased to 9.1 ± 0.2 (Fig. S10). In this acidic pH range, the predominant oxidized chlorine species were HOCl, ClO_2^- , ClO_3^- , and ClO_4^- (Fig. S11).

The electrochemical production of chlorate is typically described by the Foerster reaction (reaction 9).²⁵ This multi-step reaction involves a series of intermediate reactions that can be separated into electrochemical oxygen evolution (reaction 8) and chlorate formation (reaction 10). Although this reaction is relatively fast above pH 6.5, another pathway for chlorate formation is thought to be more important under lower pH conditions; the dismutation of hypochlorous acid to form chlorite and chloride (reaction 11), followed by rapid oxidation of chlorite by hypochlorous acid to produce chlorate (reaction 12).^{26,27}



Anodic interface potentials under these conditions ranged from 1.42 ± 0.01 V at 50 mA to 2.13 ± 0.03 V at 900 mA (Fig. 5). Results from previous studies of chlorate production on dimensionally stable anodes indicated a similar trend with chlorate production efficiency increasing until an anodic potential above which the surface kinetics of the electrode remained constant.^{28,29} One explanation for this phenomenon is a decrease in the activity of catalytically active surface sites at high anodic surface potentials.³⁰

The stepwise reactions in which chlorite is formed as an intermediate in the production of chlorate (reactions 13 and 14) may also offer an explanation for the leveling off in chlorate production rates observed above 600 mA.³¹ Standard half-cell potentials for reactions 13 and 14 were derived from tabulated thermodynamic values.³² When adjusted for the solution conditions ($T = 25^\circ\text{C}$; $\text{pH} = 3$), the half-cell reaction potentials for reactions 13 and 14 (i.e.,

+1.38 V and +1.01 V, respectively) were less positive than the anodic potential measured at any current tested (i.e., +1.42 V). While this would suggest a stepwise electrochemical mechanism for chlorate formation can occur even at low currents, this does not account for the high overpotential for the direct oxidation of HOCl (reaction 3). It has been proposed that an interface potential greater than +1.8 V is necessary to directly oxidize hypochlorous acid to chlorite (reaction 13)²⁷, which could rapidly oxidize to chlorate (reaction 14). If this stepwise pathway predominated, it could explain the leveling off of chlorate production after 600 mA, when the anodic interface potential exceeds 1.9 V.



Under the conditions at which the separated cell was tested against the undivided cell (i.e., 150 mA), the anodic overpotential would not have been sufficiently high for the aforementioned stepwise electrochemical pathway to predominate. In this instance the dismutation of hypochlorous acid described by reactions 10-12 was probably more important. In addition, reactions 10-12 produce protons, suggesting equilibrium shifts towards hypochlorous acid at lower pH values. This may help to explain why less chlorate was formed in the separated cell compared to the undivided cell, which remained at a near neutral pH throughout the electrolysis period (Fig. S4).

It is important to recognize that chlorate formation occurs only in the anolyte chamber. Therefore, the final concentration of chlorate after dilution of the anolyte solution into the collected drinking water (catholyte effluent + concentrated chlorine solution) will be less than the World Health Organization's provisional guideline value of 0.7 mg L⁻¹.¹⁹ For example, the highest concentration of chlorate measured in this study, 11.0 ± 1.8 mg L⁻¹ (i.e., [Cl⁻]₀ = 200 mg L⁻¹, ρ_q = 2160 C L⁻¹, Section 3.4) (Fig. S12), occurred at a free chlorine concentration of 319 ± 14 mg L⁻¹; after dilution of this stock solution to achieve a disinfectant concentration of 2 mg Cl₂ L⁻¹, the chlorate concentration would be 0.069 mg L⁻¹ (i.e., less than 10% of the WHO guideline value).

3.4 Effects of Chloride Concentration on System Performance

The effects of varying initial chloride concentrations were tested to provide insight into the performance of the separated cell design in source waters of varying ionic composition (Fig. S13). The lowest chloride concentration tested (i.e., 10 mg L⁻¹) was typical of inland surface water sources, whereas the highest chloride concentration (i.e., 200 mg L⁻¹) approached the US Environmental Protection Agency's secondary maximum contaminant level taste threshold of 250 mg L⁻¹. To avoid confounding effects related to voltage, the ionic strength for each test was held constant at 7 mM, with Na₂SO₄ serving as the background electrolyte (Table 1).

A linear relationship was observed between free chlorine production rate and chloride concentration (Fig. 6) between 10 and 150 mg Cl⁻ L⁻¹:

$$\frac{d[\text{Cl}_2]}{dt \times A} = (0.039 \text{ L A}^{-1} \text{ min}^{-1})[\text{Cl}^-]_0 \quad (10 \text{ mg L}^{-1} \leq [\text{Cl}^-]_0 \leq 150 \text{ mg L}^{-1}) \quad (15)$$

where $\frac{d[\text{Cl}_2]}{dt \times A}$ is the rate of free chlorine production ($\text{mg Cl}_2 \text{ A}^{-1} \text{ min}^{-1}$) and $[\text{Cl}^-]_0$ is the initial chloride concentration (mg L^{-1}) of the feed water. At $200 \text{ mg L}^{-1} \text{ Cl}^-$, free chlorine production was about 10% higher than the value predicted by extrapolation of the trend observed at lower chloride concentrations. We predict that under dilute solution conditions and low chloride concentrations, nearly 40% of mass transfer of chloride is controlled by diffusion away from the anode surface, while chloride concentrations above $150 \text{ mg L}^{-1} \text{ Cl}^-$ migration to the anode surface controls transfer (a detailed discussion of these calculations can be found in Text S3) (Fig. S14).

The Coulombic efficiency varied linearly as a function of initial chloride concentration, ranging from $2.42 \pm 0.12 \%$ for $10 \text{ mg L}^{-1} \text{ Cl}^-$ and $40.7 \pm 1.1 \%$ for $200 \text{ mg L}^{-1} \text{ Cl}^-$ (Fig. S15):

$$\varphi = 0.178[\text{Cl}^-]_0 \quad (10 \text{ mg L}^{-1} \leq [\text{Cl}^-]_0 \leq 150 \text{ mg L}^{-1}) \quad (16)$$

where φ is the Coulombic efficiency (%) of chlorine evolution at the anode and $[\text{Cl}^-]_0$ is the initial chloride concentration (mg L^{-1}) of the feed water. The effect of chloride concentrations on chlorine evolution efficiency help explain the large variability in energy consumption. The energy consumption decreased from $0.96 \pm 0.11 \text{ kWh m}^{-3}$ at 10 mg L^{-1} to $0.050 \pm 0.003 \text{ kWh m}^{-3}$ at 200 mg L^{-1} (Fig. S16). The total cell potential varied by less than 20% between the different conditions (Fig. S17), indicating chloride content was responsible for the differences in energy requirements, not solution conductivity alone.

3.5 System Performance in Samples from Representative Water Sources

Representative source water samples (Table S1) were tested in the separated cell to assess the efficacy of the system under conditions likely to be encountered in the environment. Free chlorine production rates were $1.03 \pm 0.03 \text{ mg Cl}_2 \text{ A}^{-1} \text{ min}^{-1}$ for the surface water and $2.87 \pm 0.24 \text{ mg Cl}_2 \text{ A}^{-1} \text{ min}^{-1}$ for the groundwater (Fig. 7). The predicted rates based on equation 15 for the chloride concentrations in the surface water and groundwater (i.e., $0.24 \text{ mg Cl}_2 \text{ A}^{-1} \text{ min}^{-1}$ and $2.96 \text{ mg Cl}_2 \text{ A}^{-1} \text{ min}^{-1}$, respectively) were within 5% of the experimental values for the groundwater samples, while the observed chlorine production rate for the surface water was over four times higher than the predicted value. Likewise, the coulombic efficiency estimated from equation 16 agreed with that measured for groundwater (13.4% compared to $12.1\% \pm 1.8\%$) but were much lower than the efficiency measured for surface water (1.1% compared to $4.8\% \pm 0.4\%$).

The deviation from the model prediction for chlorine evolution in surface water may have been attributable to its relatively low conductivity. The data used to establish the relationships in equations 15 and 16 were collected at an ionic strength of 7 mM with Na_2SO_4 serving as the background electrolyte, whereas the ionic strength of the surface water was approximately 2.5 mM, with substantial amount of chloride, calcium and magnesium. In the latter case, chloride-to-sulfate ratio was much greater than that of the

solution used to derive the relationship; thus, chloride carried a greater portion of current which resulted in faster rates of mass transfer of chloride towards the anode. Additionally, this low conductivity resulted in relatively high cell potentials (i.e., the initial potential was nearly 40 V, which dropped to 27 V during the one-hour electrolysis period; Fig. S18). As a result, the energy needed to produce $2 \text{ mg Cl}_2 \text{ L}^{-1}$ in the surface water was $1.8 \pm 0.1 \text{ kWh m}^{-3}$, while that for groundwater was $0.14 \pm 0.01 \text{ kWh m}^{-3}$. These results suggest that retaining a portion of the anolyte to maintain higher salt concentrations in the cell when treating low conductivity waters may be particularly beneficial.

4. Conclusions

The introduction of an anion exchange membrane into an electrochlorinator system operated with the anolyte in batch and the catholyte in continuous flow modes resulted in enhanced chlorine production and lower energy consumption from natural source waters and representative electrolyte solutions. This new design outperformed an analogous undivided cell electrochlorinator in all metrics. In addition, periods of high voltage were avoided by recycling a fraction of the finished anolyte for each subsequent run. Chlorate production also was reduced due to the acidic solution conditions of the anolyte. The system succeeded in producing ample free chlorine over a range of chloride concentrations and solution conditions.

Our results demonstrate the technology's ability to generate an adequate quantity of free chlorine for disinfection from chloride present in a source water. As is the case whenever chlorine is used to disinfect water, the presence of high concentrations of natural organic matter and bromide could result in the production of a suite of disinfection byproducts.³³ Approaches used to predict and control the formation of these compounds in electrochlorinators would be much like those used when chlorine is added from a stock solution. Extended use of this system may result in electrode and membrane fouling from calcium- and magnesium-containing precipitates formed under the basic pH conditions encountered in the catholyte. One method to avoid fouling would be to periodically wash the cathode chamber and lines with acidic anolyte (which would also help minimize biofouling). In addition, certain types of anion exchange membranes might be damaged by extended contact with chlorine produced in the anolyte, necessitating the use of chlorine-resistant membranes. To facilitate adoption of this technology, further research is necessary to minimize user interaction and the need to determine dilution levels for the concentrated disinfectant solution, including determination of flow rate and applied current combinations necessary for automated operation.

Supplementary Material

Refer to Web version on PubMed Central for supplementary material.

Acknowledgements

The authors would like to thank Dr. Siva Rama Satyam Bandaru for his assistance in the construction of the electrochemical cells used in this study and the many helpful discussions on electrochemical phenomena. We would also like to thank Dr. Amy Pickering for her insight into POU chlorinators and the complexity of their practical

application in rural settings. This study was supported by the US NIEHS Superfund Research Program (grant no. P42 ES004705).

References

- (1). UNICEF; WHO. Progress on Drinking Water, Sanitation and Hygiene. Who 2019, 1–66. 10.1111/tmi.12329.
- (2). WHO. WHO Global Water, Sanitation and Hygiene. 2018, 2018–2019.
- (3). Montgomery MA; Elimelech M Water and Sanitation in Developing Countries: Including Health in the Equation - Millions Suffer from Preventable Illnesses and Die Every Year. *Environ. Sci. Technol* 2007, 41 (1), 17–24. 10.1021/es072435t. [PubMed: 17265923]
- (4). Pooi CK; Ng HY Review of Low-Cost Point-of-Use Water Treatment Systems for Developing Communities. *npj Clean Water* 2018, 1 (1). 10.1038/s41545-018-0011-0.
- (5). Meierhofer R; Wietlisbach B; Matiko C Influence of Container Cleanliness, Container Disinfection with Chlorine, and Container Handling on Recontamination of Water Collected from a Water Kiosk in a Kenyan Slum. *J. Water Health* 2019, 17 (2), 308–317. 10.2166/wh.2019.282. [PubMed: 30942780]
- (6). Rufener S; Mäusezahl D; Mosler HJ; Weingartner R Quality of Drinking-Water at Source and Point-of Consumption-Drinking Cup as a High Potential Recontamination Risk: A Field Study in Bolivia. *J. Heal. Popul. Nutr* 2010, 28 (1), 34–41. 10.3329/jhpn.v28i1.4521.
- (7). Gärtner N; Germann L; Wanyama K; Ouma H; Meierhofer R Keeping Water from Kiosks Clean: Strategies for Reducing Recontamination during Transport and Storage in Eastern Uganda. *Water Res. X* 2021, 10. 10.1016/j.wroa.2020.100079.
- (8). Peter-Varbanets M; Zurbrügg C; Swartz C; Pronk W Decentralized Systems for Potable Water and the Potential of Membrane Technology. *Water Res.* 2009, 43 (2), 245–265. 10.1016/j.watres.2008.10.030. [PubMed: 19010511]
- (9). Pickering AJ; Crider Y; Amin N; Bauza V; Unicomb L; Davis J; Luby SP Differences in Field Effectiveness and Adoption between a Novel Automated Chlorination System and Household Manual Chlorination of Drinking Water in Dhaka, Bangladesh: A Randomized Controlled Trial. *PLoS One* 2015, 10 (3), 1–16. 10.1371/journal.pone.0118397.
- (10). Ribeiro MR; de Abreu LC; Laporta GZ Drinking Water and Rural Schools in the Western Amazon: An Environmental Intervention Study. *PeerJ* 2018, 2018 (6), 1–16. 10.7717/peerj.4993.
- (11). Rayner J; Yates T; Lantagne D; Joseph M Sustained Effectiveness of Automatic Chlorinators Installed in Community-Scale Water Distribution Systems during an Emergency Recovery Project in Haiti. *J. Water Sanit. Hyg. Dev* 2016, 6 (4), 602–612. 10.2166/washdev.2016.068.
- (12). Albert J; Luoto J; Levine D End-User Preferences for and Performance of Competing POU Water Treatment Technologies among the Rural Poor of Kenya. *Environ. Sci. Technol* 2010, 44 (12), 4426–4432. 10.1021/es1000566. [PubMed: 20446726]
- (13). Karlsson RKB; Cornell A Selectivity between Oxygen and Chlorine Evolution in the Chlor-Alkali and Chlorate Processes. *Chem. Rev* 2016, 116 (5), 2982–3028. 10.1021/acs.chemrev.5b00389. [PubMed: 26879761]
- (14). Otter P; Sattler W; Grischek T; Jaskolski M; Mey E; Ulmer N; Grossmann P; Matthias F; Malakar P; Goldmaier A; et al. Economic Evaluation of Water Supply Systems Operated with Solar-Driven Electro-Chlorination in Rural Regions in Nepal, Egypt and Tanzania. *Water Res.* 2020, 187, 116384. 10.1016/j.watres.2020.116384. [PubMed: 32980605]
- (15). Micangeli A; Michelangeli E; Naso V; Iannuzzo N The Potential in Water Supply and Sanitation Services of the on Site Production of Sodium Hypochlorite (OSEC) Driven by PV Solar Source. *J. Sustain. Dev. Energy, Water Environ. Syst* 2013, 1 (4), 311–325. 10.13044/j.sdwes.2013.01.0024.
- (16). California Water Boards. GAMA Groundwater Information System Map. 2020.
- (17). Barazesh JM; Hennebel T; Jasper JT; Sedlak DL Modular Advanced Oxidation Process Enabled by Cathodic Hydrogen Peroxide Production. *Environ. Sci. Technol* 2015, 49 (12), 7391–7399. 10.1021/acs.est.5b01254. [PubMed: 26039560]

- (18). Standard Methods for the Examination of Water and Wastewater; Rice EW, Baird RB, Eaton AD, Eds.; American Public Health Association, American Water Works Association, Water Environment Federation: Washington, DC, 2017.
- (19). Guidelines for Drinking-Water Quality, 4th ed.; World Health Organization, Ed.; 2011.
- (20). Otter P; Malakar P; Sandhu C; Grischek T; Sharma SK; Kimothi PC; Nüske G; Wagner M; Goldmaier A; Benz F Combination of River Bank Filtration and Solar-Driven Electro-Chlorination Assuring Safe Drinking Water Supply for River Bound Communities in India. *Water (Switzerland)* 2019, 11 (1). 10.3390/w11010122.
- (21). Otter P; Hertel S; Ansari J; Lara E; Cano R; Arias C; Gregersen P; Grischek T; Benz F; Goldmaier A; et al. Disinfection for Decentralized Wastewater Reuse in Rural Areas through Wetlands and Solar Driven Onsite Chlorination. *Sci. Total Environ* 2020, 721, 137595. 10.1016/j.scitotenv.2020.137595. [PubMed: 32208224]
- (22). Jaskolski M; Schmitz L; Otter P; Pellegrino Z Solar-Powered Drinking Water Purification in the Oases of Egypt's Western Desert. *J. Photonics Energy* 2019, 9 (04), 1. 10.1117/1.JPE.9.043107.
- (23). Kraft A; Blaschke M; Kreysig D; Sandt B; Schröder F; Rennau J Electrochemical Water Disinfection. Part II: Hypochlorite Production from Potable Water, Chlorine Consumption and the Problem of Calcareous Deposits. *J. Appl. Electrochem* 1999, 29 (8), 895–902. 10.1023/A:1003654305490.
- (24). Hand S; Cusick RD Electrochemical Disinfection in Water and Wastewater Treatment: Identifying Impacts of Water Quality and Operating Conditions on Performance. *Environ. Sci. Technol* 2021, 55 (6), 3470–3482. 10.1021/acs.est.0c06254. [PubMed: 33616403]
- (25). Viswanathan K; Tilak BV Chemical, Electrochemical, and Technological Aspects of Sodium Chlorate Manufacture. *J. Electrochem. Soc* 1984, 131 (7), 1551–1559. 10.1149/1.2115908.
- (26). Jung YJ; Baek KW; Oh BS; Kang JW An Investigation of the Formation of Chlorate and Perchlorate during Electrolysis Using Pt/Ti Electrodes: The Effects of PH and Reactive Oxygen Species and the Results of Kinetic Studies. *Water Res.* 2010, 44 (18), 5345–5355. 10.1016/j.watres.2010.06.029. [PubMed: 20619871]
- (27). Czarnetzki LR; Janssen LJJ Formation of Hypochlorite, Chlorate and Oxygen during NaCl Electrolysis from Alkaline Solutions at an RuO₂/TiO₂ Anode. *J. Appl. Electrochem* 1992, 22 (4), 315–324. 10.1007/BF01092683.
- (28). Cornell A; Håkansson B; Lindbergh G Ruthenium-Based Dimensionally Stable Anode in Chlorate Electrolysis. *J. Electrochem. Soc* 2003, 150 (1), D6. 10.1149/1.1522386.
- (29). Eberil' VI; Fedotova NS; Novikov EA; Mazanko AF Studying the Link between the Potential of a Metal-Oxide Anode, the Current Efficiency for Chlorate, and the Current Losses for the Oxygen and Chlorine Evolution in a Wide Range of the Chlorate Electrolysis Conditions. *Russ. J. Electrochem* 2000, 36 (12), 1296–1302. 10.1023/A:1026603714489.
- (30). Nylén L; Cornell A Critical Anode Potential in the Chlorate Process. *J. Electrochem. Soc* 2006, 153 (1), D14. 10.1149/1.2135216.
- (31). Tasaka A; Tojo T Anodic Oxidation Mechanism of Hypochlorite Ion on Platinum Electrode in Alkaline Solution. *J. Electrochem. Soc* 1985, 132 (8), 1855–1859. 10.1149/1.2114230.
- (32). Reed JJ Digitizing “The NBS Tables of Chemical Thermodynamic Properties: Selected Values for Inorganic and C1 and C2 Organic Substances in SI Units”1. *Journal of Research of the National Institute of Standards and Technology.* 2020. 10.6028/JRES.125.007.
- (33). Deborde M; von Gunten U Reactions of Chlorine with Inorganic and Organic Compounds during Water Treatment-Kinetics and Mechanisms: A Critical Review. *Water Res.* 2008, 42 (1–2), 13–51. 10.1016/j.watres.2007.07.025. [PubMed: 17915284]

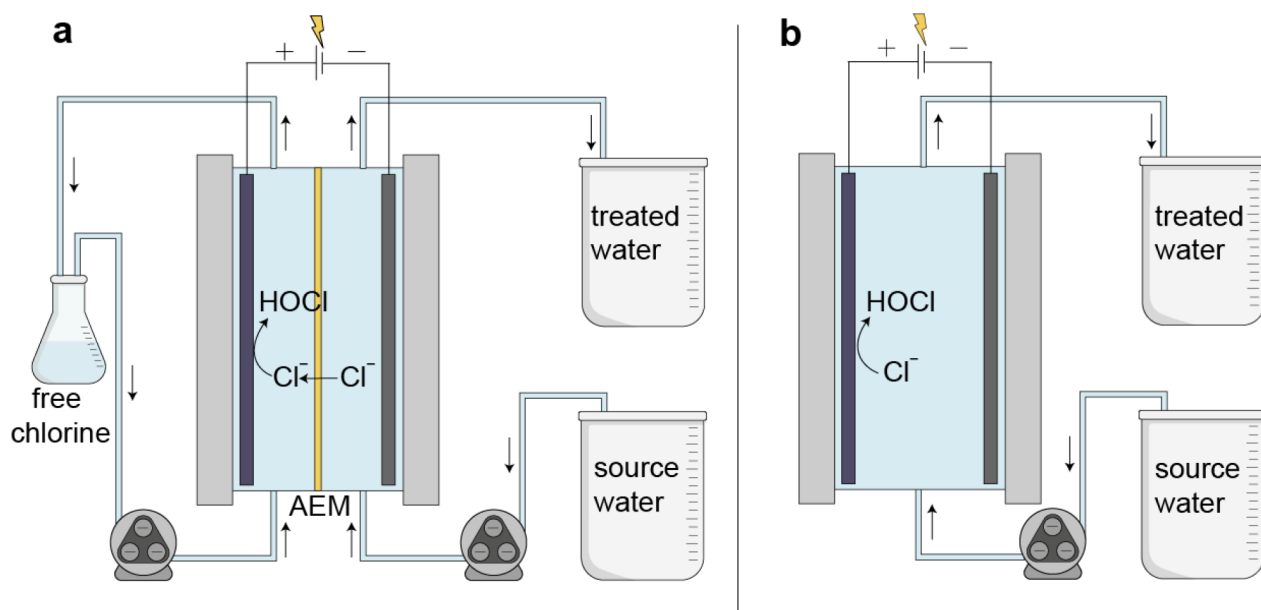


Fig. 1 -.
Flow schematic of a) separated cell and b) undivided cell (AEM = anion exchange membrane).

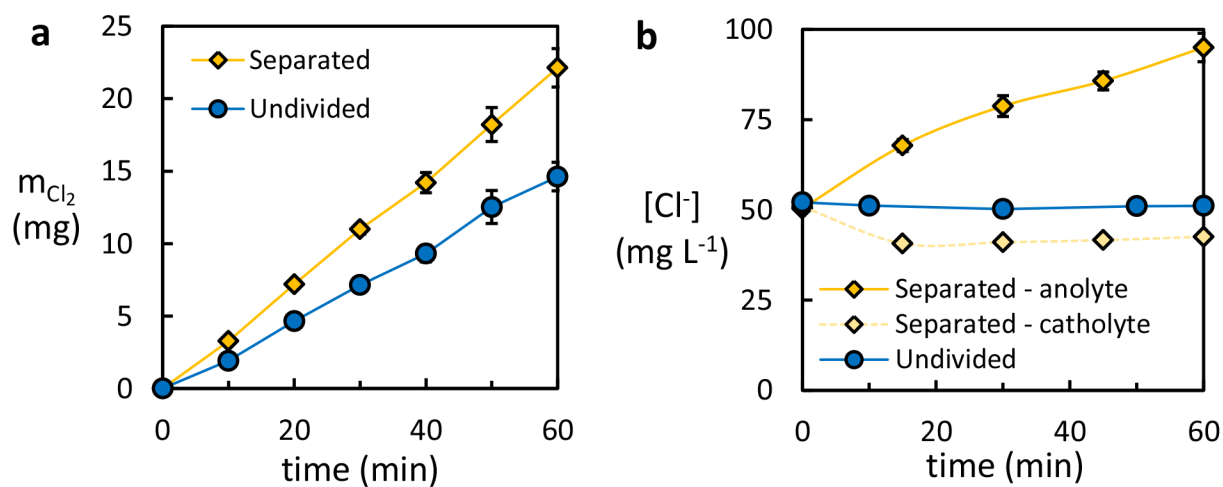


Fig. 2 -.

(a) Total mass of free chlorine generated and (b) chloride concentrations over time for two cell configurations with a $50 \text{ mg L}^{-1} Cl^-$ solution. Total free chlorine is reported in mass units because the undivided cell did not contain an anolyte chamber. Time is used instead of charge density because the definition presented in equation 4 does not apply to the undivided cell. See Table 1 “Cells comparison & recycled anolyte” for electrolyte composition.

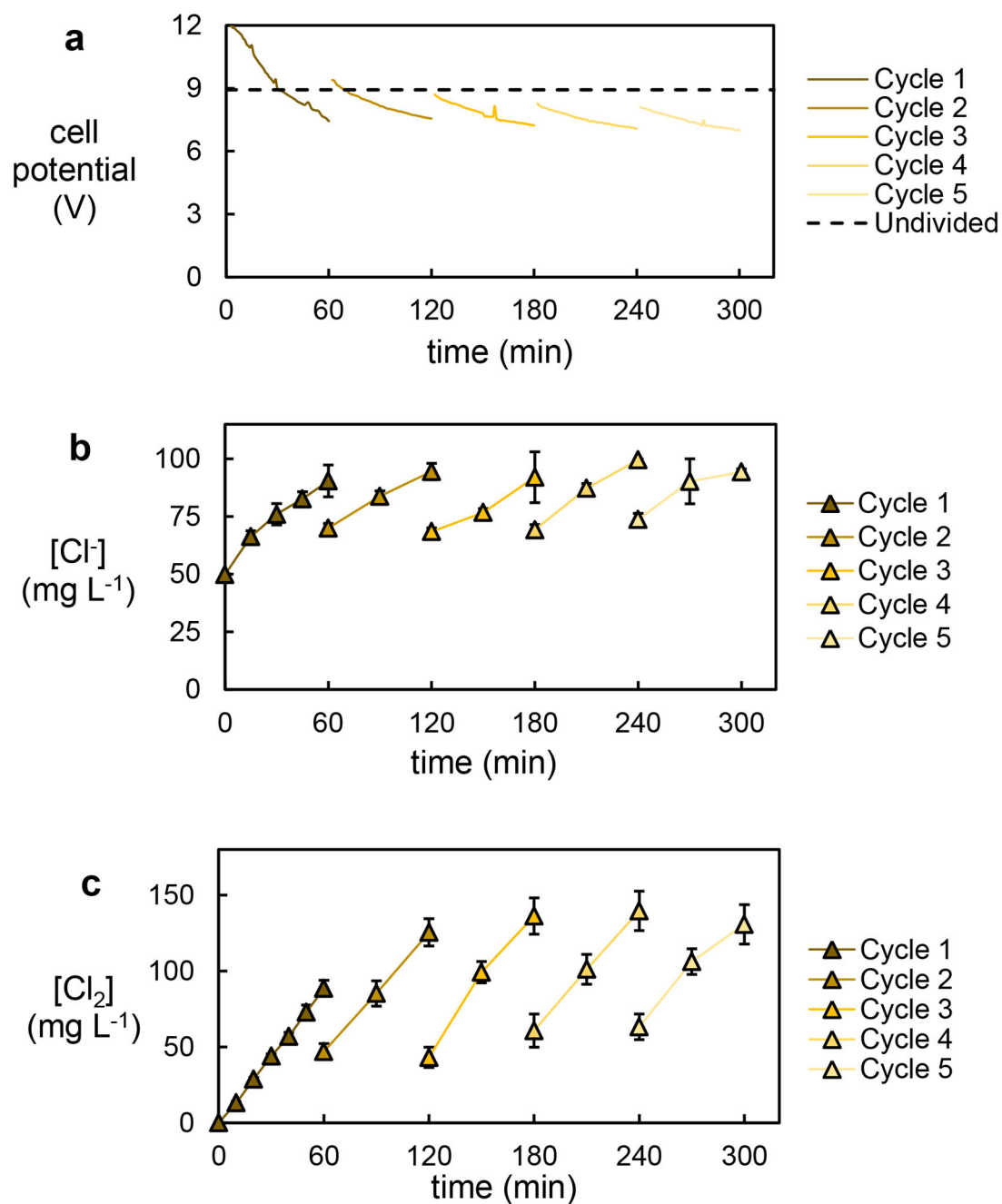


Fig. 3 –.

The (a) cell potential, (b) chloride concentration, and (c) chlorine concentration of the separated cell in recycled anolyte mode for five sequential cycles. The average potential of the undivided cell is plotted for reference. See Table 1 “Three cells comparison & recycled anolyte” for electrolyte composition.

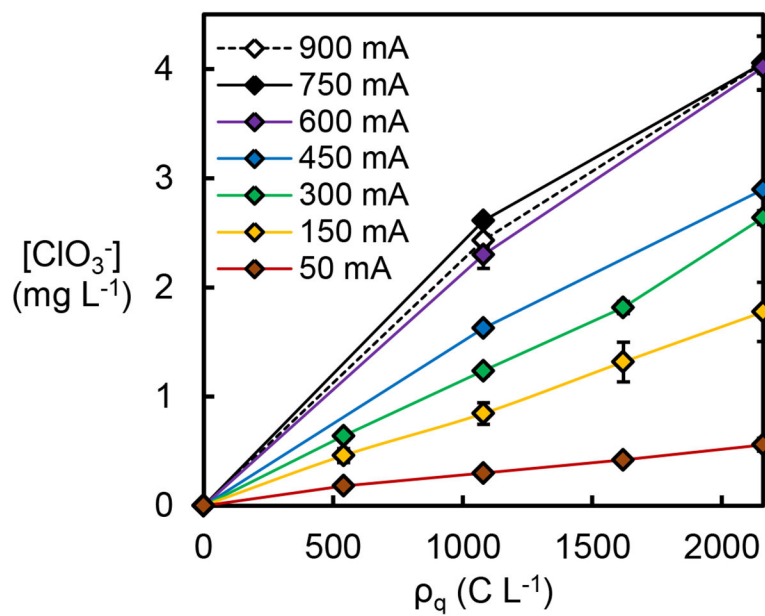


Fig. 4 –.
Chlorate concentration in anolyte of separated cell under varying applied currents. See Table 1 “Variable current” for electrolyte composition.

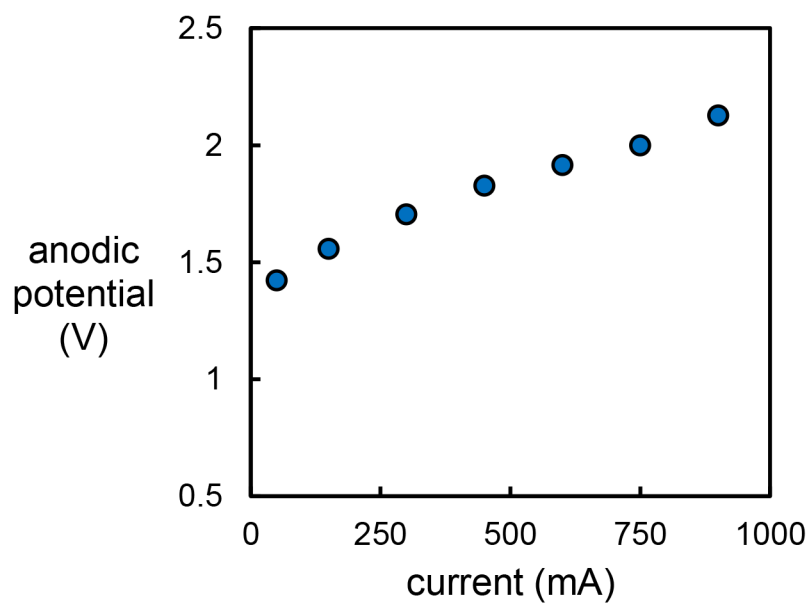


Fig. 5 -. Anodic interface potential as a function of applied current. Measured with a Ag/AgCl reference electrode and reported vs SHE. ($[\text{NaCl}] = 1.41 \text{ mM}$, $[\text{NaHCO}_3] = 1.5 \text{ mM}$, and $[\text{Na}_2\text{SO}_4] = 1 \text{ M}$ as a background electrolyte.)

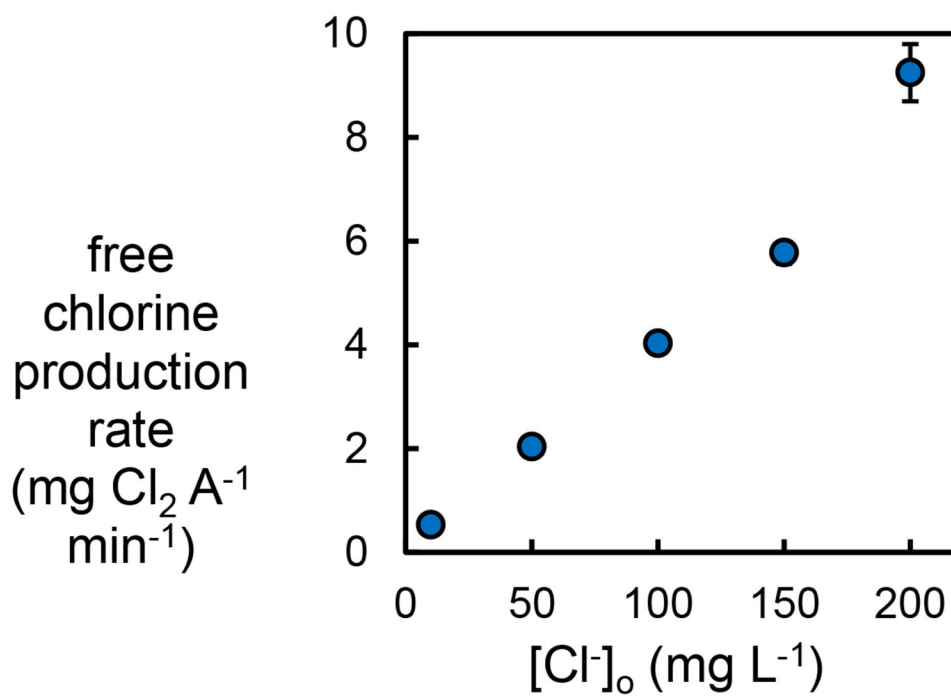


Fig. 6 -. Free chlorine production rate of chlorine evolution as a function of chloride concentration. See Table 1 “Variable chloride” for electrolyte composition.

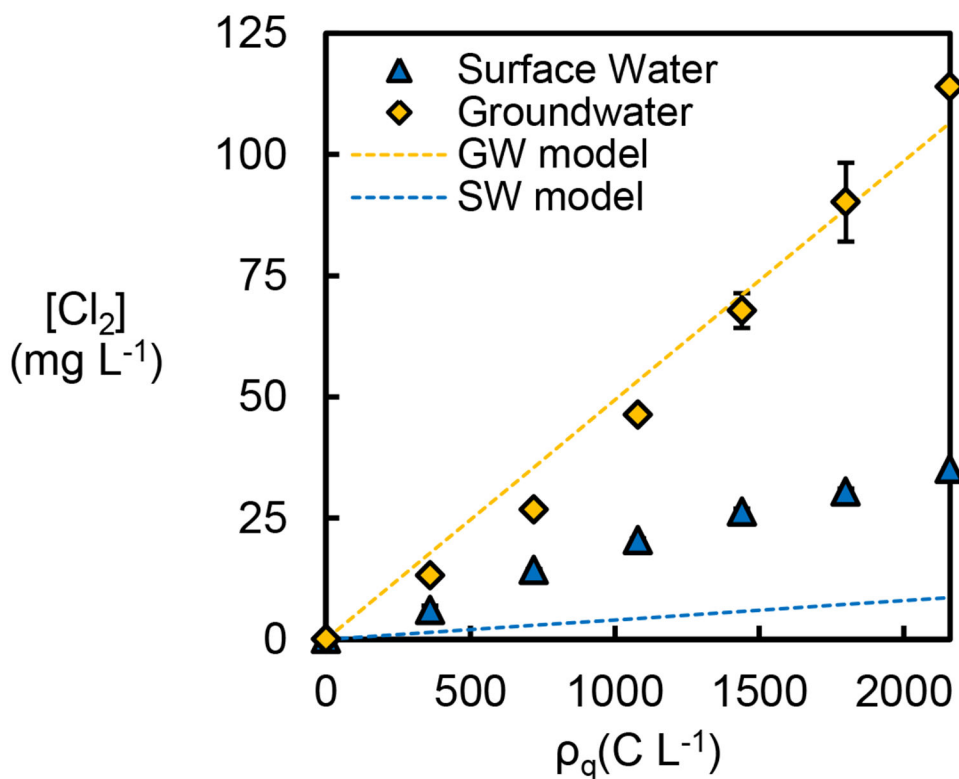


Fig. 7 –.

Free chlorine production from surface water and groundwater. The dashed lines were calculated from the model presented in equation 15, factoring in an applied current of 150 mA, an anolyte volume of 250 mL, and initial chloride concentrations of 6.1 mg L⁻¹ and 75.5 mg L⁻¹ for surface water and groundwater, respectively. See Table S1 for composition of the natural water samples.

Table 1.

Synthetic electrolytes used in chlorine production experiments.

Experiments	Ionic Strength (mM)	NaCl (mM)	NaHCO ₃ (mM)	Na ₂ SO ₄ (mM)	Current (mA)
Cells comparison & recycled anolyte	7.0	1.41	1.5	1.35	150
Variable current	7.0	1.41	1.5	1.35	50 - 900
Variable chloride					
10 ppm	7.0	0.28	1.0	1.92	300
50 ppm	7.0	1.41	1.0	1.53	300
100 ppm	7.0	2.82	1.0	1.06	300
150 ppm	7.0	4.23	1.0	0.59	300
200 ppm	7.0	5.64	1.0	0.40	300